ORNLMIT218

NTIS
One Source. One Search. One Solution.

DISPERSION IN A TAPERED FLUIDIZED BED

MASSACHUSETTS INST. OF TECH., OAK RIDGE, TENN. SCHOOL OF CHEMICAL ENGINEERING PRACTICE

20 OCT 1975

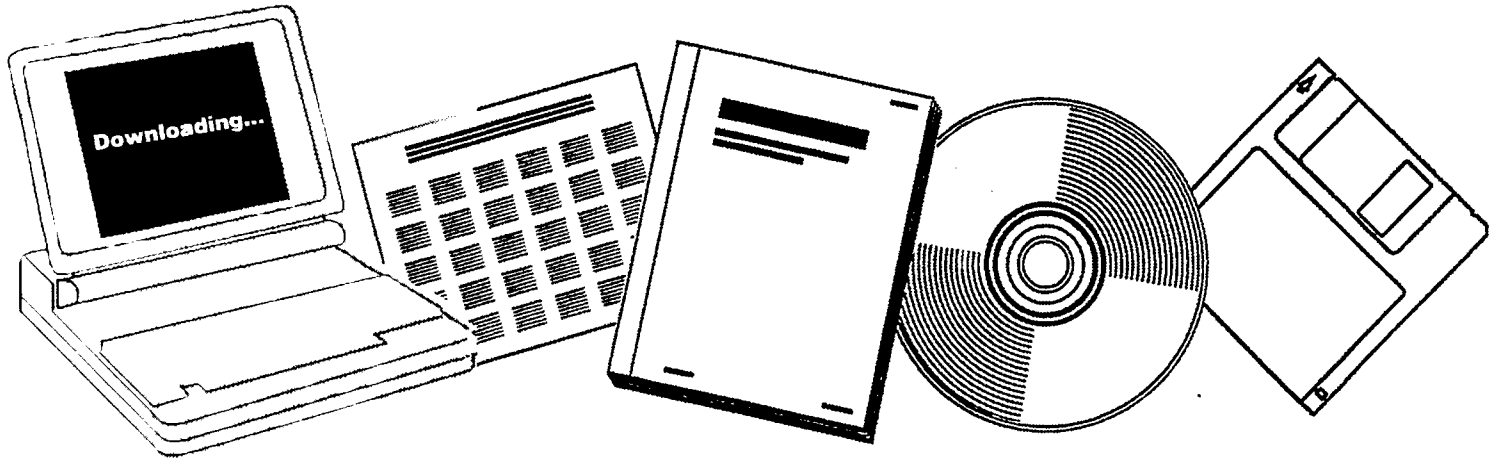

U.S. Department of Commerce
National Technical Information Service

One Source. One Search. One Solution.

NTIS

Providing Permanent, Easy Access to U.S. Government Information

National Technical Information Service is the nation's largest repository and disseminator of government-initiated scientific, technical, engineering, and related business information. The NTIS collection includes almost 3,000,000 information products in a variety of formats: electronic download, online access, CD-ROM, magnetic tape, diskette, multimedia, microfiche and paper.

Search the NTIS Database from 1990 forward

NTIS has upgraded its bibliographic database system and has made all entries since 1990 searchable on **www.ntis.gov.** You now have access to information on more than 600,000 government research information products from this web site.

Link to Full Text Documents at Government Web Sites

Because many Government agencies have their most recent reports available on their own web site, we have added links directly to these reports. When available, you will see a link on the right side of the bibliographic screen.

Download Publications (1997 - Present)

NTIS can now provides the full text of reports as downloadable PDF files. This means that when an agency stops maintaining a report on the web, NTIS will offer a downloadable version. There is a nominal fee for each download for most publications.

For more information visit our website:

www.ntis.gov

U.S. DEPARTMENT OF COMMERCE
Technology Administration
National Technical Information Service
Springfield, VA 22161

ORNLMIT218

OAK RIDGE NATIONAL LABORATORY
OPERATED BY
UNION CARBIDE CORPORATION
NUCLEAR DIVISION

POST OFFICE BOX X
OAK RIDGE, TENNESSEE 37830

ORNL/MIT-218

DATE: October 20, 1975 COPY NO.

SUBJECT: Dispersion in a Tapered Fluidized Bed

AUTHOR: A.S. Lee, F. Gutierrez, S. Khosrowshahi, and R.M. Schlapfer

Consultant: C.W. Hancher

MASTER

ABSTRACT

Dispersion in a 2-in.-ID cylindrical column and a tapered column, 1-in.-ID at the bottom, 3-in.-ID at the top, and 42-in. long, was measured experimentally with a dye tracer injection technique. Dispersion measurements in both columns were taken with single phase (water) flow and with two-phase flow (alumina or glass packing fluidized in water). Parameters varied during dispersion measurements were flow rate, bed height, and packing. The dispersion coefficient was calculated at each operating condition for both columns from equations presented by Levenspiel. The inverse Peclet number and vessel dispersion number were calculated and compared for both columns.

NOTICE
This report was prepared as an account of work sponsored by the United States Government. Neither the United States nor the United States Energy Research and Development Administration, nor any of their employees, nor any of their contractors, subcontractors, or their employees, makes any warranty, express or implied, or assumes any legal liability or responsibility for the accuracy, completeness or usefulness of any information, apparatus, product or process disclosed, or represents that its use would not infringe privately owned rights.

Oak Ridge Station
School of Chemical Engineering Practice
Massachusetts Institute of Technology

Contents

		Page
1.	Summary	4
2.	Introduction	4
	2.1 Background	4
	2.2 Theory	5
	2.3 Previous Work	7
	2.3.1 Dispersion in Round Tubes	7
	2.3.2 Theoretical Treatment of a Tracer Pulse	12
	2.3.3 Tapered Columns	12
	2.4 Objectives	13
	2.5 Method of Attack	13
3.	Apparatus and Procedure	14
	3.1 Apparatus	14
	3.2 Procedure	14
4.	Results and Discussion of Results	16
	4.1 Experimental Results	16
	4.1.1 Cylindrical Column	16
	4.1.2 Tapered Column	23
	4.2 Theoretical Results	31
5.	Conclusions	33
6.	Recommendations	34
7.	Acknowledgement	34
8.	Appendix	35
	8.1 The Effective Diameter of a Conical Section	35
	8.2 Sample Calculations	35
	8.3 Location of Data	38
	8.4 Nomenclature	38
	8.5 Literature References	39

1. SUMMARY

Liquid-solid tapered fluidized beds have been proposed as bioreactors to prevent biomass accumulation and to allow continuous operation. A tapered column may offer more stability and a wider range of operating conditions than a cylindrical column.

Backmixing in both cylindrical and tapered fluidized beds was measured experimentally. The experimental apparatus consisted of a 42-in.-long tapered column with 1-in. ID at the bottom and 3-in. ID at the top. A 2-in.-ID cylindrical column of approximately equal volume was also studied for comparison with the tapered column. One-tenth millimeter glass and -70+100 mesh alumina packings were fluidized with water in both columns. A dye tracer was injected at the bottom of each column. The residence time distribution at various operating conditions was recorded by means of a movable photocell. The dispersion coefficient was calculated for each column by techniques presented by Levenspiel. For this and all other calculations, the effective diameter of the tapered column was taken to be the diameter of a cylindrical column of equal height and equal volume.

The vessel dispersion number, the dispersion coefficient, and the inverse Peclet number are presented graphically for different operating conditions. The vessel dispersion number and the inverse Peclet number decreased with increasing flow rates, while the dispersion coefficient increased with increasing flow rates in both columns with and without solids.

2. INTRODUCTION

2.1 Background

A solid-liquid fluidized bed is a bed of solid particles suspended by an upward flow of liquid. The principal application of these contactors is as catalytic reactors with liquid reactants and a solid catalyst or as a bioreactor to contact immobilized biological or biochemical species with liquid streams. This technique offers advantages over fixed bed operations including higher reaction rates due to the higher specific area of small particles and easier replacement of solids during operation. Therefore, investigations have begun to determine the mixing characteristics of the fluidized beds (6, 7, 8, 12). Both cylindrical and tapered (conical) fluidized beds are being investigated. Because of the narrow range of operating conditions and the unstable flow patterns at higher flow rates in a conventional fluidized bed, a better column design is needed. To remedy such problems and to attain stable operating conditions, a tapered column concept has been proposed.

2.2 Theory

Elements of fluid taking different routes through a reactor may require different lengths of time to transit the reactor. The distribution of these times for a stream of fluid is called the residence time distribution of fluid. Dye tracer injected into liquid can be used to determine this residence time distribution. For an input tracer signal, the downstream response is represented by a concentration-time curve. This curve of tracer concentration as a function of time at any particular location is called the C-curve. An idealized instantaneous pulse of tracer in the stream entering a vessel, called a Dirac delta function, is represented mathematically by

$$\delta(t - t_o) = \infty \text{ at } t = t_o \tag{1}$$

$$\delta(t - t_o) = 0 \text{ elsewhere} \tag{2}$$

such that

$$\int_{-\infty}^{\infty} \delta(t - t_o)dt = 1 \tag{3}$$

The mean value or the centroid of the response to this inlet pulse is a measure of the average residence time expressed by:

$$\bar{t} = \frac{\int_0^{\infty} tCdt}{\int_0^{\infty} Cdt} \tag{4}$$

If the response curve is only known at a number of discrete time values, then the mean time is approximated by

$$\bar{t} \cong \frac{\sum_i t_i C_i \Delta t_i}{\sum_i C_i \Delta t_i} \tag{5}$$

The most important quantity in describing dispersion is the variance or spread of the response defined as

$$\sigma^2 = \frac{\int_0^\infty (t - \bar{t})^2 C dt}{\int_0^\infty C dt} \tag{6}$$

or

$$\sigma^2 = \frac{\int_0^\infty t^2 C dt}{\int_0^\infty C dt} - \bar{t}^2 \tag{7}$$

If only discrete values are known, the variance may be approximated as

$$\sigma^2 \simeq \frac{\sum_i t_i^2 C_i \Delta t_i}{\sum_i C_i \Delta t_i} - \bar{t}^2 \tag{8}$$

The variance is proportional to the square of the spread of the distribution and has the units of $(\text{time})^2$.

For any particular vessel, through which fluid flows at steady state, the C-curve response is the same for identical tracer injections. The flow pattern inside the vessel determines the tracer response curve obtained at the outlet. Many types of models can be used to characterize non-ideal flow within vessels. Analogies are usually drawn between mixing in actual flow and a diffusional process. These are called dispersion models. Dispersion refers to the effective transport of tracer due to radial diffusion, axial diffusion, and redistribution of tracer due to gradients of the velocity profile.

Dispersion for a stagnant fluid is described by the phenomenological equation,

$$\frac{\partial C}{\partial t} = D \frac{\partial^2 C}{\partial Z^2} \tag{9}$$

where D is the dispersion coefficient. Dispersion may alternatively be described in terms of a chain or network of ideal mixers, or various flow regions connected in series or parallel. Dispersion models for real systems usually describe deviation from either plug flow or ideal mixed flow.

2.3 Previous Work

2.3.1 Dispersion in Round Tubes

For laminar flow in round, smooth tubes, Taylor (14) showed that dispersion due to molecular diffusion and radial velocity variations may be characterized by an effective axial dispersion coefficient:

$$D = \frac{d^2U^2}{192D_v} \tag{10}$$

Taylor neglected axial molecular diffusion and established the limiting condition for negligible radial dispersion as

$$\frac{L}{U} >> \frac{d^2}{28.8\ D_v} \tag{11}$$

In Taylor's analysis, longitudinal mixing was assumed to be caused solely by the parabolic velocity distribution of laminar flow in long pipes with no end effects. Taylor experimentally determined the stream velocity by measuring the conductivity-time curve of the brine which he injected into a tube through which water was flowing.

Aris (1) later showed that the axial effect of dispersion and diffusion were additive.

$$D_L' = D_v + \frac{d^2U^2}{192D_v} \tag{12}$$

He concluded that "1/192", above, by Taylor was a function of the tube shape and velocity profile. Both Aris (2) and Taylor (15) concluded that an effective axial dispersion coefficient D_L' can also be used for turbulent flow. This coefficient is a function of the Fanning friction factor.

Cairns and Prausnitz (5) studied the longitudinal mixing in fluidized beds with a salt solution tracer technique. They found that longitudinal mixing properties are strongly affected by particle concentration; and are also functions of particle density and fluid velocity profiles.

Levenspiel and Smith (11) showed that a dimensionless parameter, the Peclet number, can be used as the similarity criterion for longitudinal mixing. In this model dispersion was determined for a frame of reference moving with velocity equal to the average fluid velocity. The moving fluid

model is then obtained by transforming the moving frame of reference to a stationary frame of reference.

The solution to Eq. (9) by Levenspiel is given in dimensionless form for open vessels by

$$C_\theta = \frac{1}{2\sqrt{\pi\theta(\frac{D}{UL})}} \exp\left[-\frac{(1-\theta)^2}{4\theta(D/UL)}\right] \tag{13}$$

For closed vessels, Levenspiel solved Eq. (9) numerically and plotted concentration as a function of time as shown in Fig. 1 (10). A family of C-curves was generated with the vessel dispersion number as a parameter. From this graph, it is noted that the skewness of the C-curve increases with the vessel dispersion number, D/UL. The variance for an open vessel is determined by substitution of Eq. (13) into Eq. (6). The result is Eq. (14), where D/UL is the vessel dispersion number and is a measure of the extent of dispersion. For an open tube, with no dispersion at the inlet,

$$\frac{\sigma^2}{\bar{t}^2} = 2(\frac{D}{UL}) + 3(\frac{D}{UL})^2 \tag{14}$$

For a series of stirred tanks,

$$\frac{\sigma^2}{\bar{t}^2} = 2(\frac{D}{UL}) - 2(\frac{D}{UL})^2(1 - e^{-UL/D}) \tag{15}$$

Levenspiel (9) expressed the dispersion coefficient for dispersion of fully developed flow in long pipes in the functional form,

$$D = f_1(\rho, \mu, d_t, \epsilon, D_v) \tag{16}$$

Equation (16) can be expressed in terms of dimensionless groups:

$$\frac{D}{Ud_t} = f_2(\frac{\rho U d_t}{\mu}, \frac{\mu}{\rho D_v}, \frac{\epsilon}{d_t}) \tag{17}$$

or

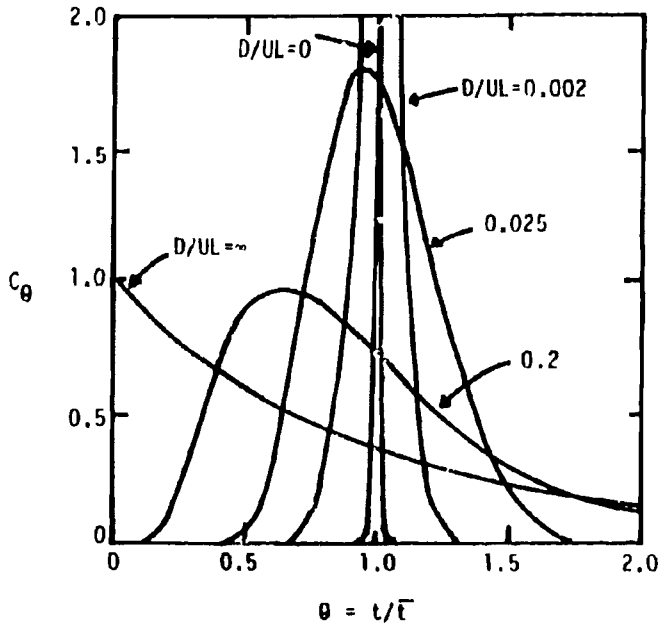

MASSACHUSETTS INSTITUTE OF TECHNOLOGY SCHOOL OF CHEMICAL ENGINEERING PRACTICE AT OAK RIDGE NATIONAL LABORATORY			
C-Curves for Closed Vessels (10)			
DATE 10-19-75	DRAWN BY FG	FILE NO. CEPS-X-218	FIG. 1

$$\frac{1}{Pe} = f_2(Re, Sc, \frac{\varepsilon}{d_t}) \tag{18}$$

where ε/d_t is the roughness number. For laminar flow, Levenspiel stated that the roughness number is not significant and Eq. (18) reduces to

$$\frac{D}{Ud_t} = f_3(Re, Sc) \tag{19}$$

The functional form of Eq. (19) agrees with Taylor's correlation, Eq. (10), which can be expressed as

$$\frac{D}{Ud_t} = \frac{1}{192}(\frac{Ud_t}{D_v}) \tag{20}$$

or

$$\frac{\varepsilon}{Ud_t} = \frac{1}{192}(\frac{\rho Ud_t}{\mu})(\frac{\mu}{\rho D_v}) \tag{21}$$

or

$$\frac{D}{Ud_t} = \frac{1}{192}(Re)(Sc) \tag{22}$$

Equation (21) is applicable to fully-developed flow in long pipes if

$$28.8 \frac{L}{d_t} > > (\frac{\rho Ud_t}{\mu})(\frac{\mu}{\rho D_v}) \tag{23}$$

For the turbulent regime, Levenspiel states that the turbulent eddy mixing overshadows the molecular diffusion in the transport of materials. The functional relationship in Eq. (18) for turbulent flow becomes,

$$\frac{D}{Ud_t} = f_4(\frac{\rho Ud_t}{\mu}, \frac{\varepsilon}{d_t}) \tag{24}$$

The experimental and theoretical results presented by Taylor and Levenspiel are shown graphically in Fig. 2.

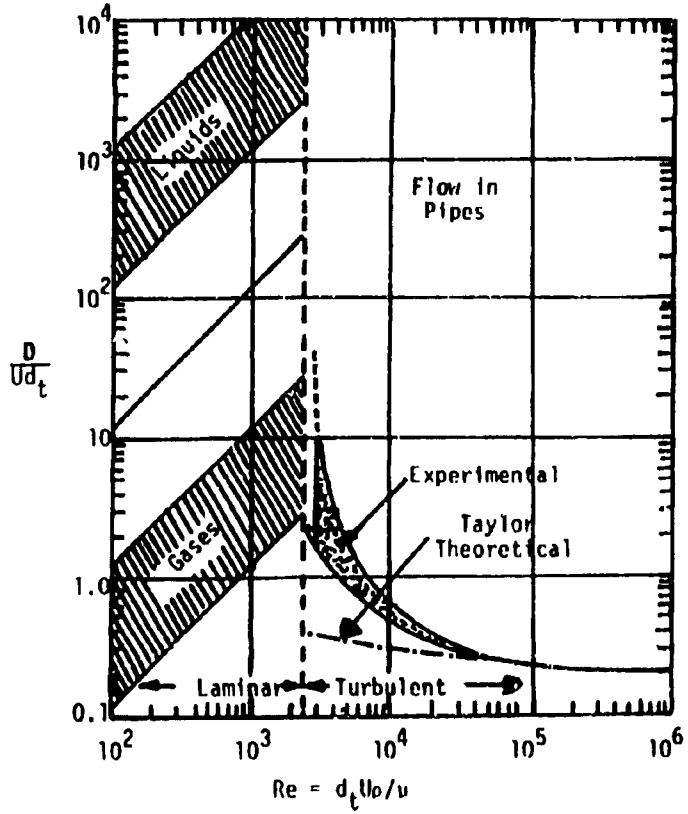

MASSACHUSETTS INSTITUTE OF TECHNOLOGY SCHOOL OF CHEMICAL ENGINEERING PRACTICE AT OAK RIDGE NATIONAL LABORATORY			
CORRELATION OF DISPERSION FOR FLUID FLOWING IN PIPES			
DATE 10-19-75	DRAWN BY SK	FILE NO. CEPS-X-218	FIG. 2

2.3.2 Theoretical Treatment of a Tracer Pulse

Van der Laan (16) treated a pulse injection to a straight column as a source term in the continuity equation of the tracer. In this model, the pipe was divided into three sections: an entrance region from negative infinity to the point of injection, the test region from the injection point to a downstream location where residence time measurements were taken, and the exit region from the downstream location to positive infinity. Each of these sections is assumed to have different dispersion characteristics. The tracer injection was represented by the Dirac delta function. In other treatments by Aris, Bischoff, and Levenspiel (1, 3, 4), the injection was treated as an arbitrary function.

2.3.3 Tapered Columns

The available literature on tapered columns is very limited. Levey et al. (12) investigated fluidized bed conversion of UO_3 to UF_4 in a tapered column. Cold enriched uranyl nitrate is converted to UO_3 by denitration, reduced to UO_2, and hydrofluorinated to a product stream of 99% UF_4. Levey obtained data for percent of bed expansion as a function of gas velocity and obtained mixing data of UO_2 into UO_3 in a continuous fluid bed for a turnover time of 3.14 hr. The turnover times were better in the tapered bed; therefore, the utilization of tapered columns in batch operation, especially for slow reactions (such as hydrofluorination of UO_2) was recommended.

Scott, Hancher, and Shumate (13) investigated a tapered fluidized bed as a bioreactor and reported bed expansion and pressure drop in a 42-in.-long tapered column, 1-in.-ID at the bottom and 3-in.-ID at the top. Calculation of overall bed properties was based on the summation of bed properties in a series of discrete bed volumes in the reactor. As predicted, pressure drop per unit length decreased with increasing flow rate after fluidization. The superficial velocity decreased with increasing height, causing the void fraction to decrease as predicted by the mathematical model.

Hancher (7) in an extension of the previous report investigated the hydraulic pressure drop for the same tapered column and a 2-in.-ID straight column. Two packings, -65+80 mesh coal and -40+80 mesh Dowex 2-X10 were fluidized for flow rates ranging from 90-1200 ml/min. Hancher concluded that the tapered fluidized bed was easier to control at any void fraction since at the top the interface was closely packed and no spouting occurred. From visual observations, vertical mixing of the solid bed appeared to be smaller in the tapered column than in the straight column. At high flow rates (above 700 ml/min), Hancher observed that the lower portion of the reactor was void of solids as predicted. Nevertheless, the bed was stable and the extent of vertical mixing appeared to be low.

2.4 Objectives

The objectives were:

1. To measure dispersion experimentally in a tapered column and in a cylindrical column with and without solids.

2. To compare the dispersion data obtained for both vessels.

3. To develop and solve the differential equation for axial dispersion in a tapered column.

4. To recommend improvements in the experimental apparatus and to make suggestions for further investigation.

2.5 Method of Attack

The dispersion for solid-liquid fluidization at various operating conditions was calculated from the variance of dye tracer responses by Eq. (8) in two Plexiglas columns, a 2-in.-ID cylindrical column and a 1- to 3-in.-ID tapered column. For this purpose, a photocell was placed at various locations up the column for liquid flow with no solids and at the top of the solids bed for two phase fluidization. The vessel dispersion number was then calculated by Eq. (14) for liquid flow in both columns. The vessel dispersion number for solid-liquid fluidization in both columns was calculated by Eq. (15). The dispersion coefficient and inverse Peclet number were then calculated from the vessel dispersion number. For the tapered column, an effective diameter based on an equal volume and equal height cylindrical column was calculated. The vessel dispersion numbers and the dispersion coefficients were graphically presented at different operating conditions.

A theoretical derivation for dispersion in a tapered bed was attempted. A differential mass balance was developed for a conical section of the bed. A stagnant fluid model assuming fluid at rest was first established for a tracer signal input represented by a Dirac delta function. The Laplace transform was applied and the resulting Bessel's equation was to be solved to obtain $\bar{C}$ as a function of position coordinate Z and transform parameter p.

A moving frame of reference relation is used to modify the stagnant fluid dispersion model to fluid flow dispersion model. The Laplace transformed concentration $\bar{C}$ is directly related to the variance of the concentration-time curve at the limit of p equal to zero in Eq. (25) (16). As a result, the dispersion coefficient is related to the variance of the concentration-time curve.

$$\sigma^2 = \left(\frac{d^2\bar{C}}{dp^2}\right)_{p\to 0} - \left(\frac{d\bar{C}}{dp}\right)^2_{p\to 0} \qquad (25)$$

or

$$\sigma^2 = \int_0^\infty \theta^2 C d\theta - \bar{\theta}^2 \qquad (26)$$

3. APPARATUS AND PROCEDURE

3.1 Apparatus

A diagram of the experimental apparatus is shown in Fig. 3. A 2-in.-ID cylindrical column and a tapered column, 1-in.-ID at the bottom, 3-in.-ID at the top, and 42-in. long, are used to determine dispersion. The water flow rate is measured by a calibrated rotameter. Rhodamine B (tetraethylrhodamine) dye tracer is injected at the bottom of the vessels by a pulse generator. The pulse generator injects approximately 10 cm^3 of a 100-ppm solution of Rhodamine B in water into the column. The distribution of the tracer at any column height is measured by a movable photocell connected to a voltmeter and a strip chart recorder.

3.2 Procedure

After establishing a water flow rate in the range of 44 to 550 ml/min, a dye pulse was injected. Initially, the four three-way valves of the pulse generator were set to direct the inlet water to the vessel and the dye solution to a drain container. The two valves in the dye stream were directed to enclose 10 cm^3 of the dye solution. Finally, the two valves in the water stream were set to flow water through the 10 cm^3 of dye, thus carrying the dye into the vessel. The dye was injected after a chart speed and an attenuation were chosen for the strip chart recorder. The chart speed ranged from 0.01 to 0.1 in./sec, and the attenuation ranged from 0.5 to 5 v. The variances and mean times were calculated from the C-curves obtained. For each set of operating conditions, three C-curve measurements were taken to check the reproducibility of the data. The water flow rate was measured at the column outlet for each run.

When backmixing was investigated for both columns with liquid flow only, the photocell was located 44, 67.4, and 120 cm above the inlet for the tapered vessel and at 32.5, 64.7, and 95 cm above the inlet for the 2-in.-ID vessel. The flow rates were varied from 44 to 550 ml/min at each height.

Two solid packings, 0.1 mm glass and -70+100 mesh alumina, were fluidized in the two columns. The weight of packing charged to the column was calculated by measuring the volume occupied by 100 g of each packing in a known volume of water. The volume occupied or the wet volume for 100 g of 0.1-mm glass is 56 ml. For -70+100 alumina, the wet volume for 100 g is

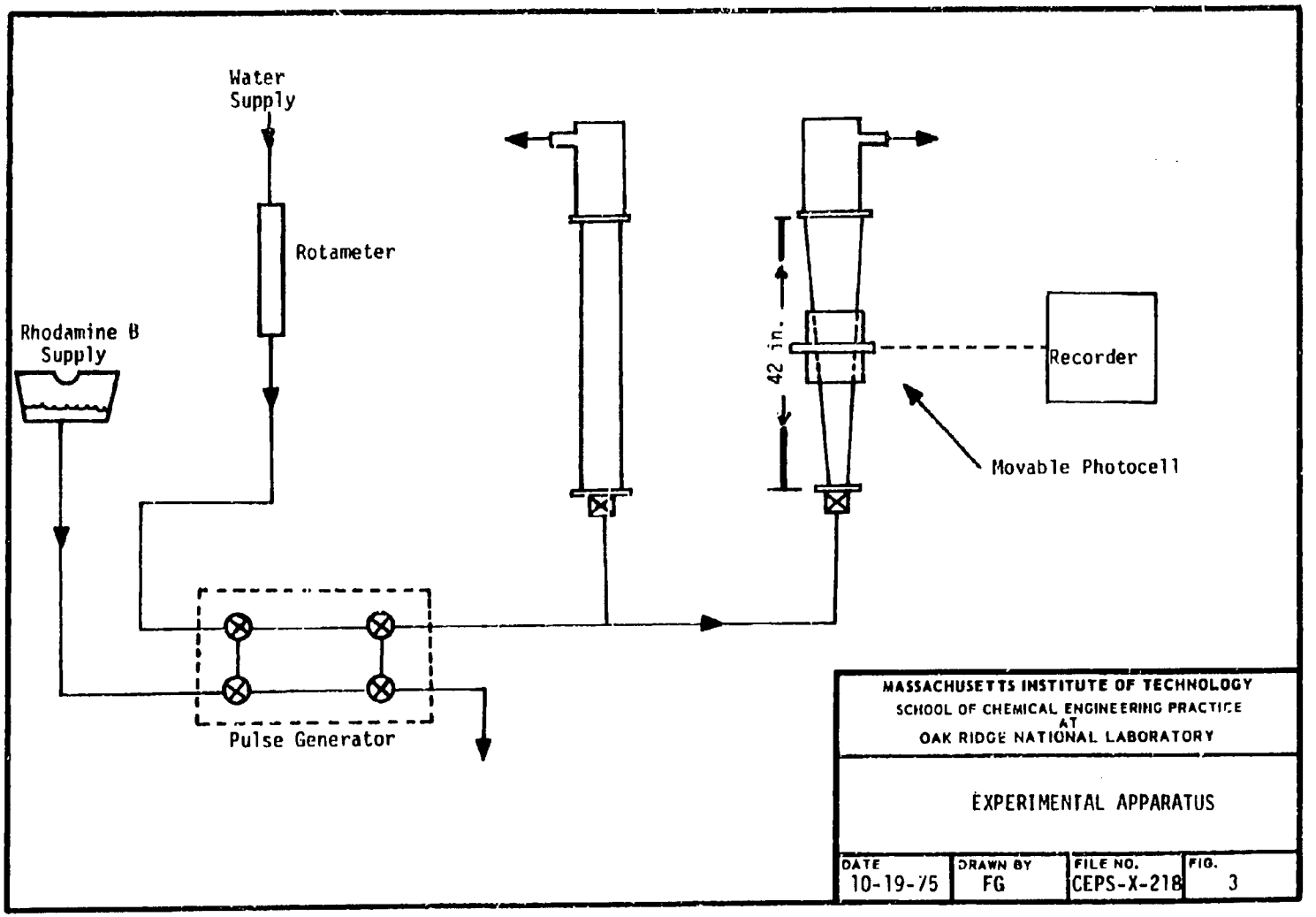
Water
Supply
Rotameter
Rhodamine B
Supply
42 in.
Recorder
Movable Photocell
Pulse Generator
MASSACHUSETTS INSTITUTE OF TECHNOLOGY
SCHOOL OF CHEMICAL ENGINEERING PRACTICE
AT
OAK RIDGE NATIONAL LABORATORY
EXPERIMENTAL APPARATUS
DATE
10-19-75
DRAWN BY
FG
FILE NO.
CEPS-X-218
FIG.
3

approximately 100 ml. From this information, one gram of 0.1-mm glass occupies 0.56 ml, and one gram of -70+100 alumina occupies 1 ml.

Four masses for each packing: 100, 150, 200, and 300 g of alumina and 196, 339, 554, and 759 g of glass, were examined in the tapered column. Dispersion measurements for each mass were obtained at five flow rates ranging from 44 to 550 ml/min. To compare equal weights of each packing in both columns, 300 g of alumina and 759 g of glass were fluidized in the 2-in.-ID vessel. In both columns, the photocell was located about 1 to 3 in. above the bed height.

4. RESULTS AND DISCUSSION OF RESULTS

4.1 Experimental Results

The vessel dispersion number, the dispersion coefficient, and the inverse Peclet number coefficient were plotted against either the Reynolds number or the flow rate for various operating conditions. Complete reproducibility was not observed at each operating condition; however, in most cases, from the three data points at a fixed operating condition, two were close to each other. The deviation may be explained by minor instabilities in flow rate causing variations in input impulses.

4.1.1 Cylindrical Column

The effect of Reynolds number on the vessel dispersion number for three locations in the 2-in.-ID column with liquid flow only is shown in Fig. 4. The vessel dispersion number which is a measure of the extent of dispersion decreases with increasing Reynolds numbers for each height. At a constant Reynolds number, the vessel dispersion number decreases with column height due to decreasing entrance effect at larger distance from entrance.

Similarly, the vessel dispersion number for the straight column packed with alumina and glass decreases with increases of Reynolds number as shown in Figs. 5 and 6. Comparison of dispersion between packed and empty columns is difficult, but if the same operating conditions are chosen, the vessel dispersion number can be compared. For example, at a flow rate of 162 ml/min, alumina fluidizes at a bed height of 32.7 cm with vessel dispersion number ranging from 0.06 to 0.13. For this flow rate in the empty column at 32.5-cm height, from Fig. 4, the vessel dispersion number ranges from 0.11 to 0.16. The lower values of vessel dispersion numbers in the packed column could indicate a flatter velocity profile. The solid particles in the fluidized bed prevent fully-developed flow and hinder dispersion.

The vessel dispersion number for glass and alumina could not be compared directly since different masses of each packing were employed in the 2-in.-ID column. The effect of flow rate on the dispersion coefficient for the 2-in. column with and without solids is shown in Figs. 7 through 9. The

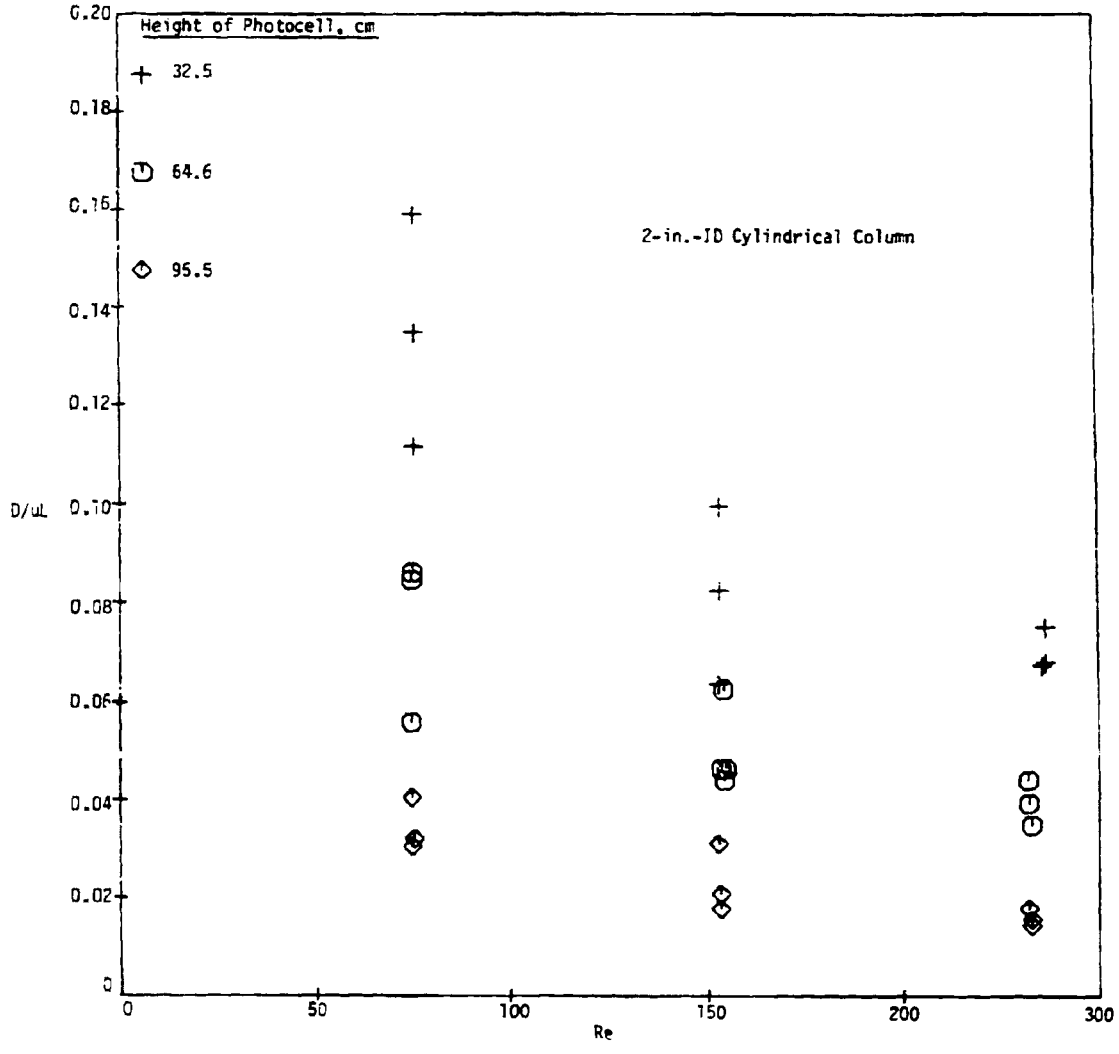

Fig. 4. Effect of Reynolds Number on Vessel Dispersion Number

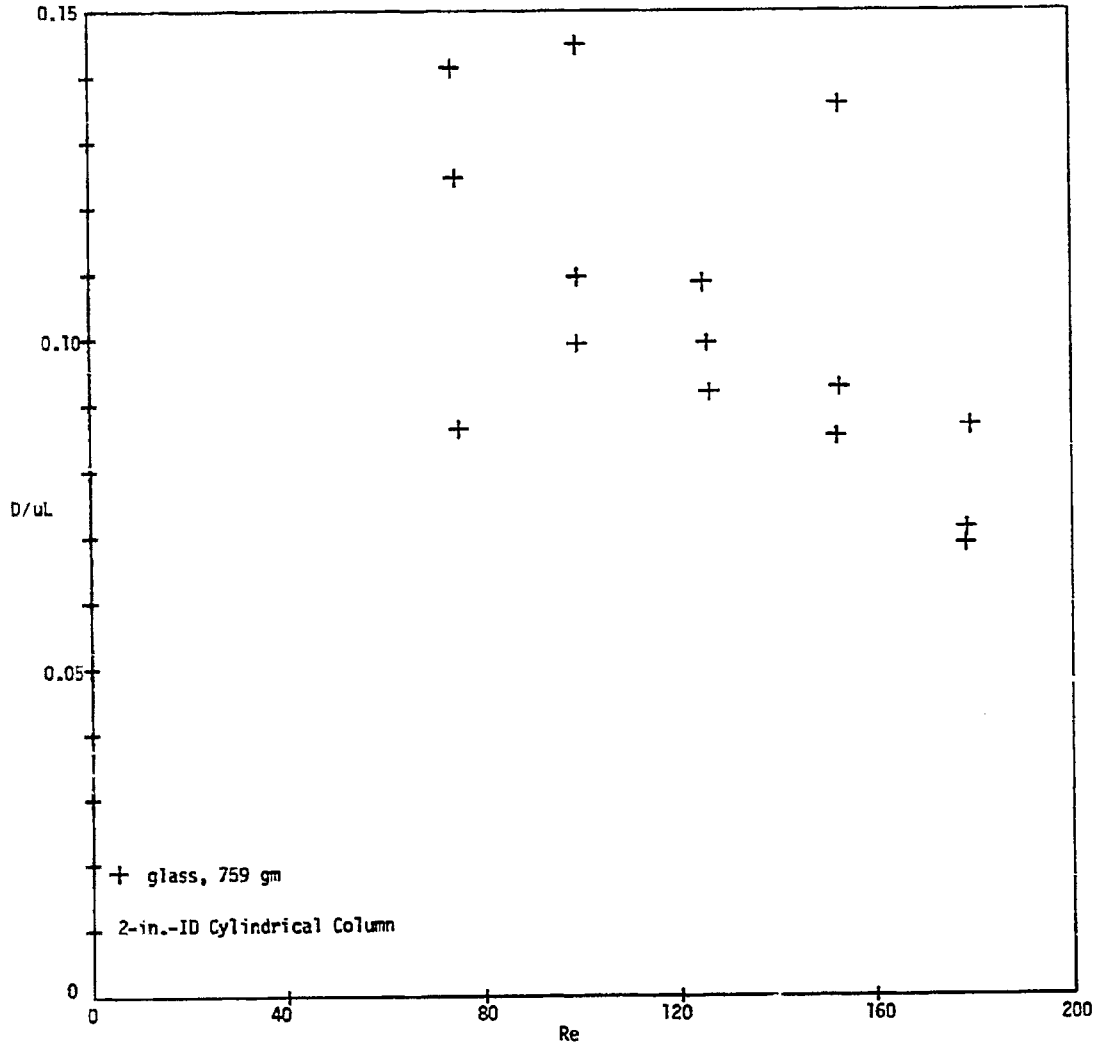

Fig. 5. Effect of Reynolds Number on Vessel Dispersion Number for Glass

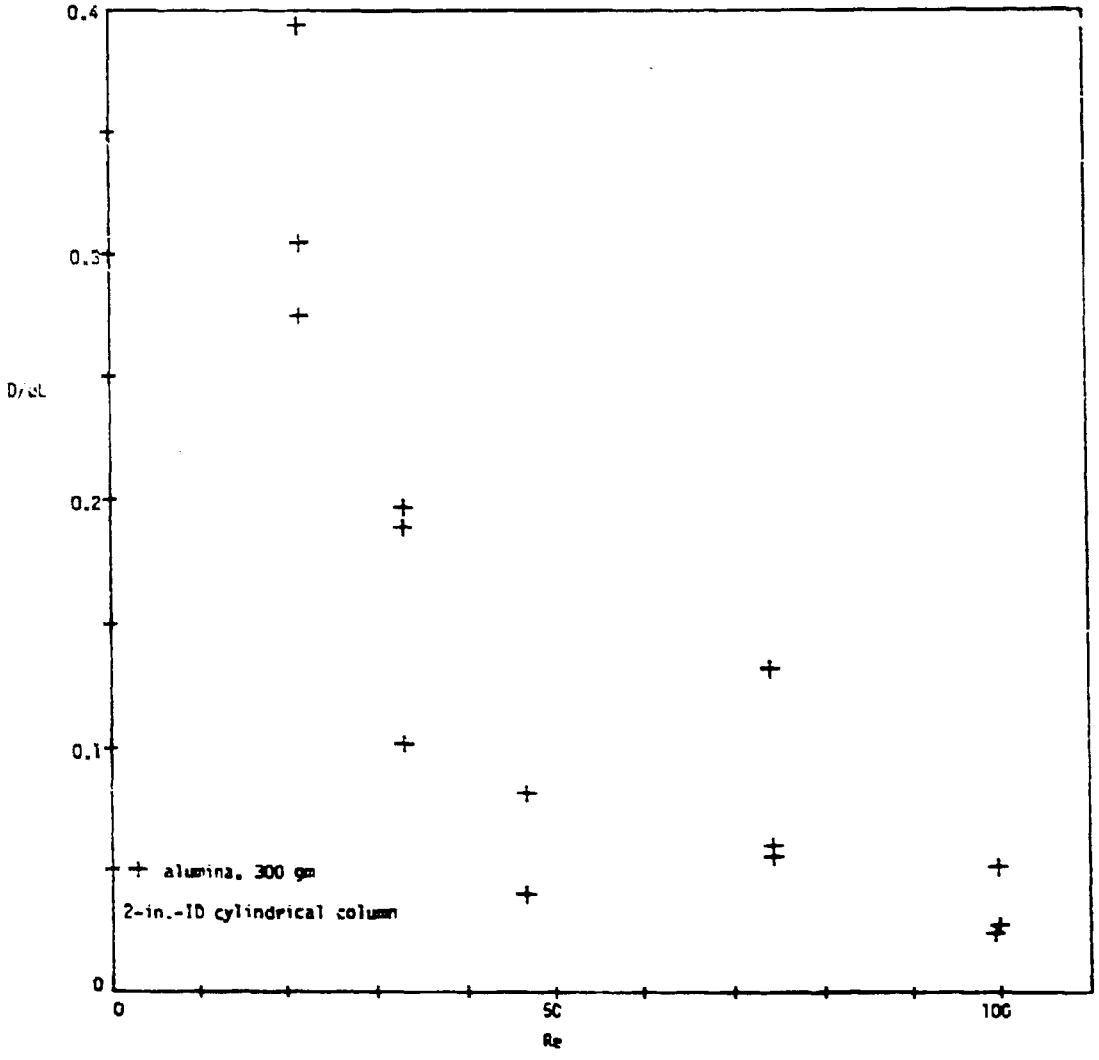

Fig. 6. Effect of Reynolds Number on Vessel Dispersion Number for Alumina

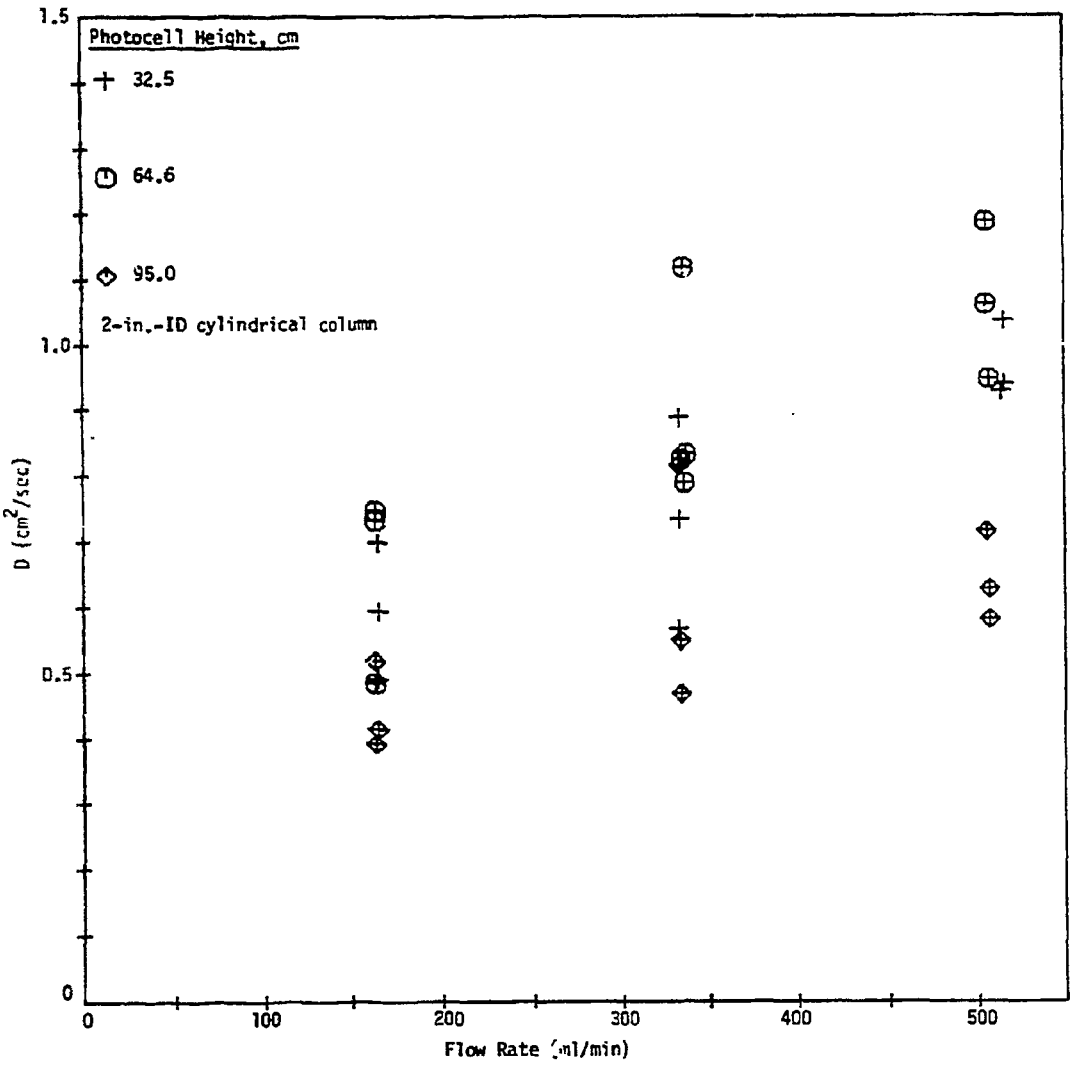

Fig. 7. Effect of Flow Rate on Dispersion Coefficient

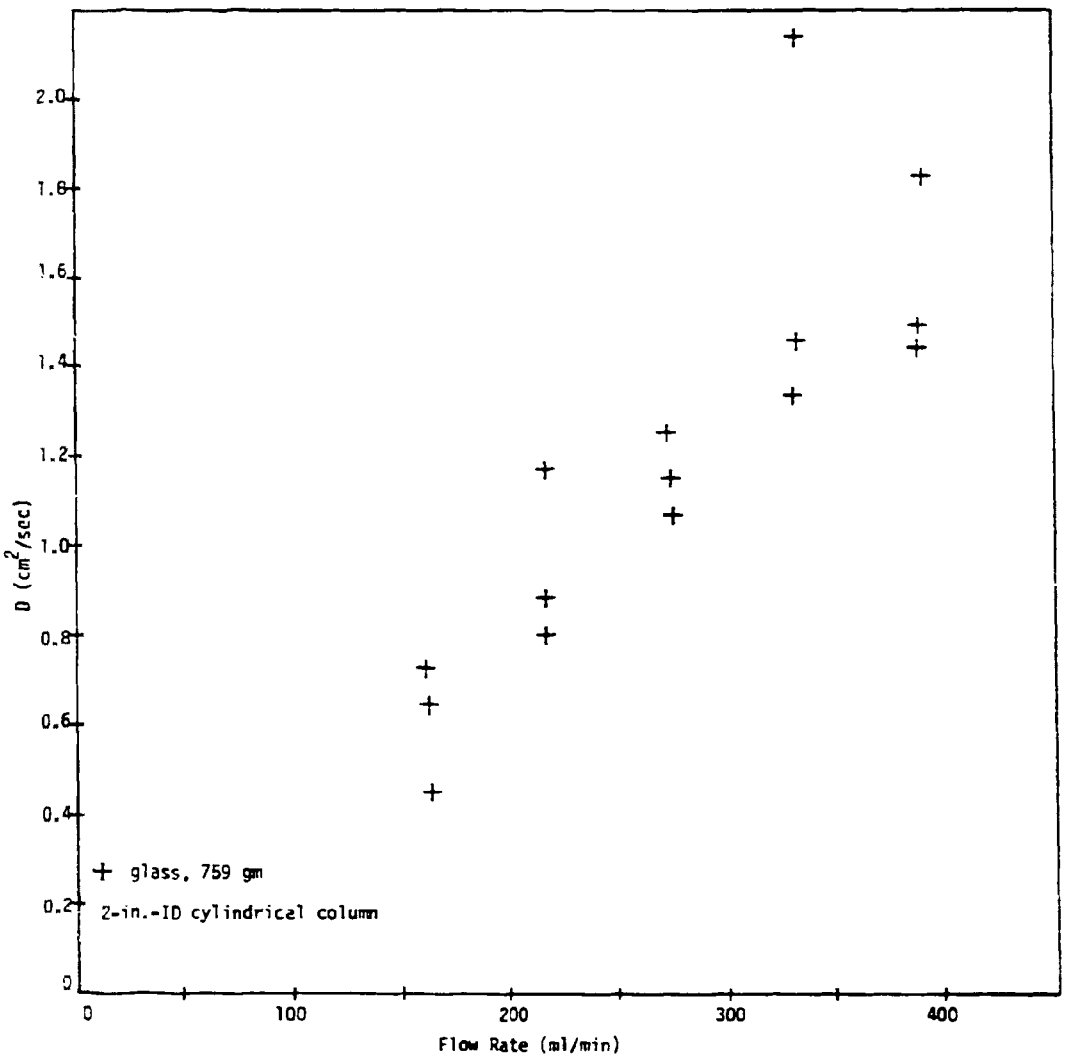

Fig. 8. Effect of Flow Rate on Dispersion Coefficient for Glass

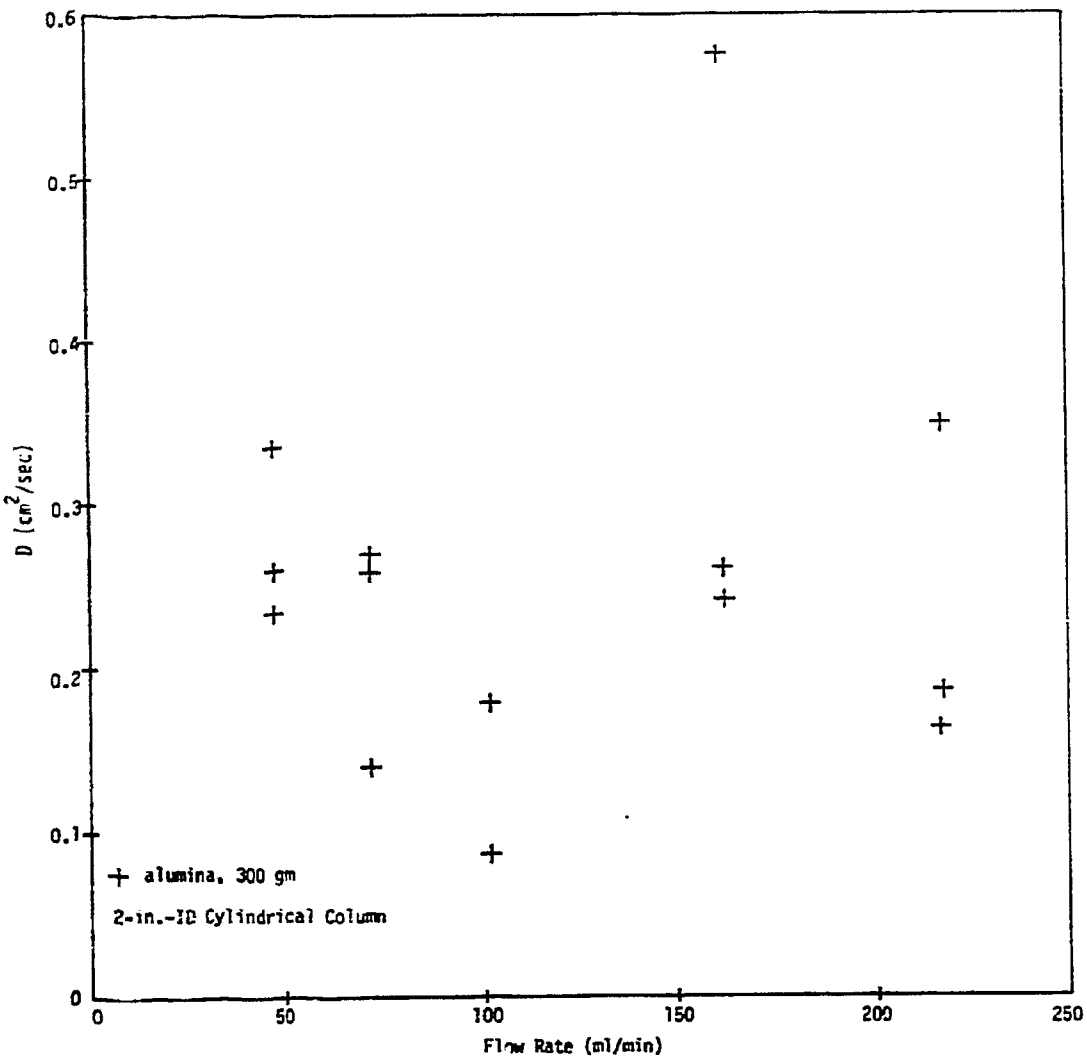

Fig. 9. Effect of Flow Rate on Dispersion Coefficient for Alumina

dispersion coefficient increases with increasing flow rate for both fluidized and single-phase flow. A comparison of the dispersion coefficients can only be performed at the same operating conditions. Insufficient data to evaluate the dispersion coefficient at fixed weight of solid make this comparison unrealistic.

The inverse Peclet number, D/Ud_t, which expresses the intensity of dispersion is also presented as a function of flow rate in Figs. 10 through 12. As shown in Figs. 10 through 12, the inverse Peclet number decreases with increasing Reynolds number with alumina and with an empty column. For glass packing, the trend cannot clearly be established as shown in Fig. 11. The downward trend is in complete disagreement with the relation reported by Levenspiel (Fig. 2) which shows a linear increase of inverse Peclet number with increases of the Reynolds number in the laminar region up to a Reynolds number of 2300. The Levenspiel distribution as shown in Fig. 2 does not apply for the operating conditions encountered, however, because Eq. (23) is not satisfied. Furthermore, in Fig. 2 an extrapolation of the Taylor's theoretical curve into the laminar region yields inverse Peclet numbers between 0.6 and 1.1 with a downward slope consistent with the present experimental data.

4.1.2 Tapered Column

An effective diameter for the tapered column which corresponded to the diameter of a cylindrical column of equal height and volume was calculated (see Appendix 8.1 for derivation). The Reynolds number and the inverse Peclet number were based on this effective diameter. As the Reynolds number increases, the tapered column vessel dispersion number decreases as shown in Fig. 13. Since the dispersion in the tapered column was modeled as the dispersion in an effective cylinder, comparison of Figs. 13 and 4 is not reasonable. This would result in a comparison of dispersion between two cylindrical columns of different diameters rather than comparison between the tapered column and the 2-in. cylindrical column. The effect of flow rate on the dispersion coefficients for two heights in the tapered column is illustrated in Fig. 14.

At a fixed height the dispersion coefficient increases with increasing flow rate. In the Levenspiel analysis of dispersion, the dispersion coefficient is assumed to be independent of height at a constant flow rate. The dispersion coefficients in Fig. 14 for the tapered column and Fig. 7 for the 2-in. cylindrical column are relatively more constant for all heights at low flow rates than at high flow rates. As shown in both these figures, the assumption that the dispersion coefficient is a constant for any height is not valid at high flow rates for the short columns studied. At any flow rate, dispersion coefficients vary more with height in the tapered column than in the 2-in. column. The assumption of constant dispersion coefficient in a tapered bed, therefore, may not be valid.

The effect of flow rate on the dispersion coefficient for various masses of alumina and glass is shown in Figs. 15 and 16. The dispersion coefficients increase with increasing flow rate for each mass of packing. At any constant flow rate, the dispersion coefficient appears to increase with bed mass and,

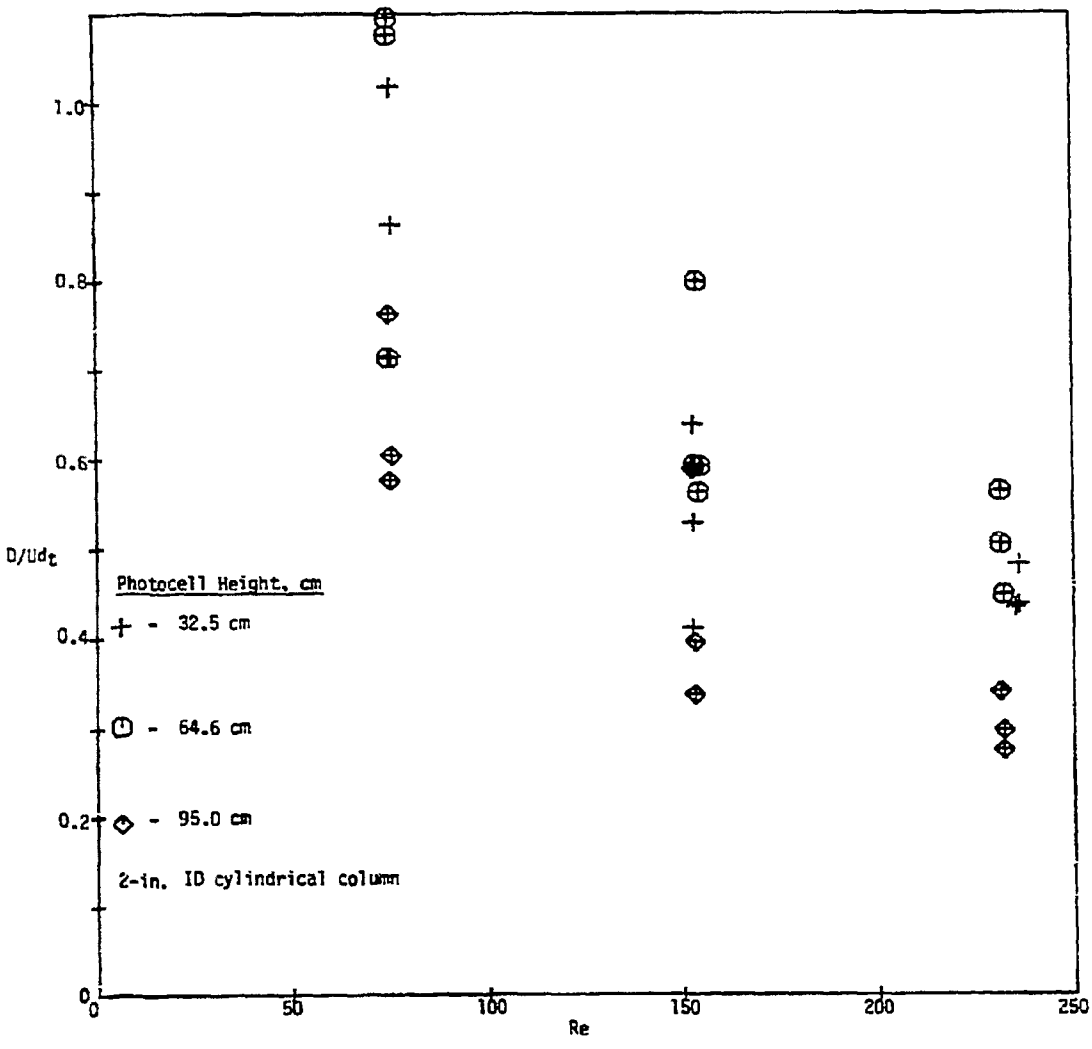

Fig. 10. Effect of Reynolds Number on Inverse Peclet Number

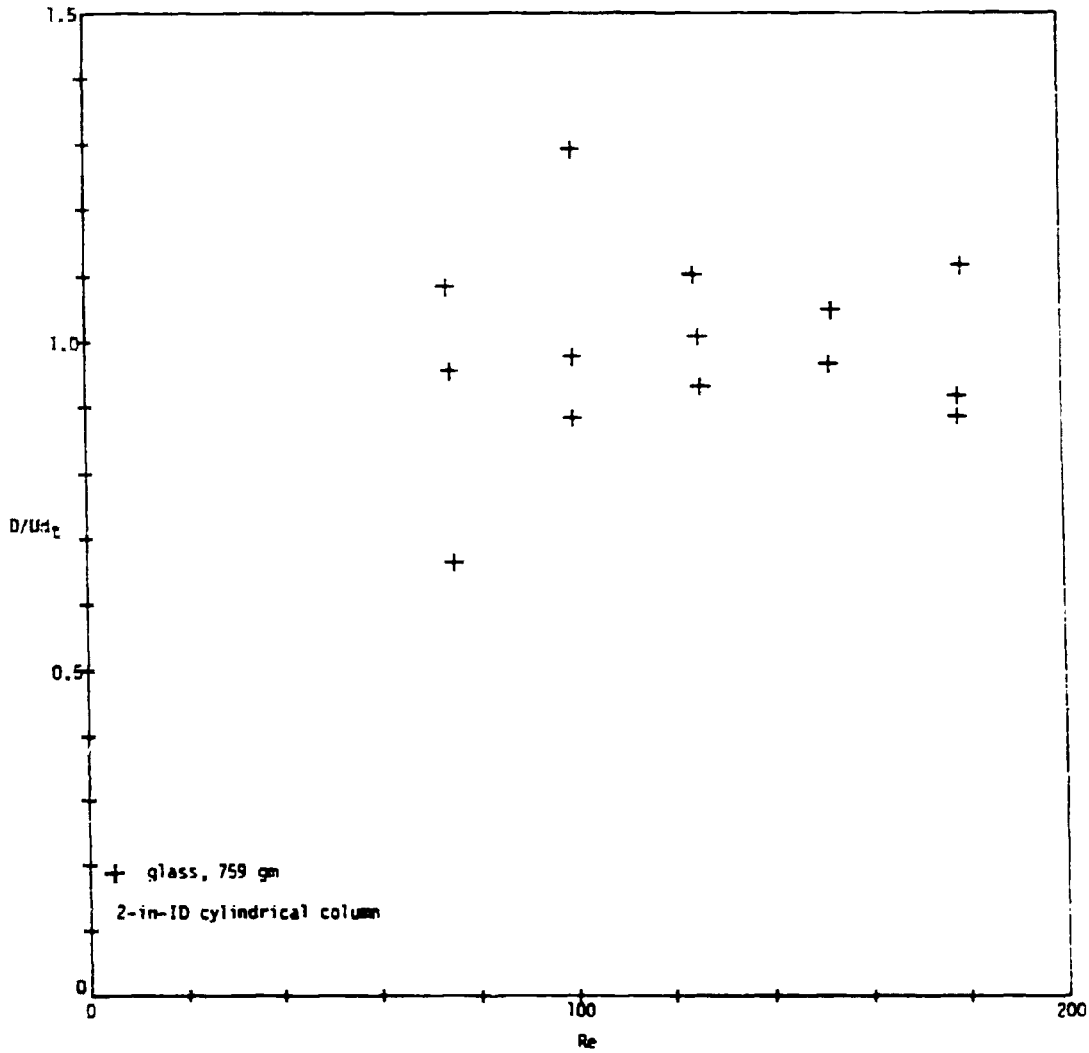

Fig. 11. Effect of Reynolds Number on Inverse Peclet Number for Glass

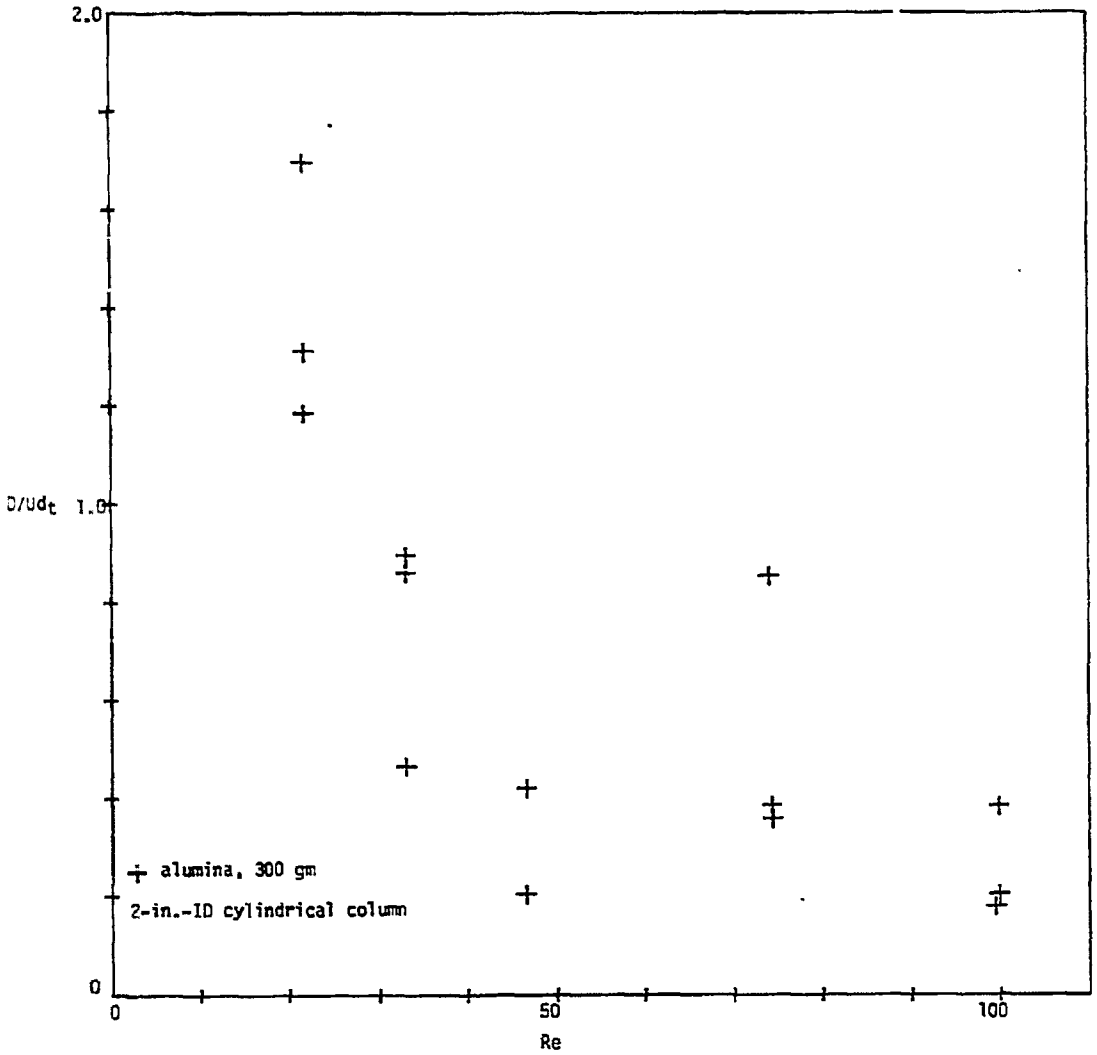

Fig. 12. Effect of Reynolds Number on Inverse Peclet Number for Alumina

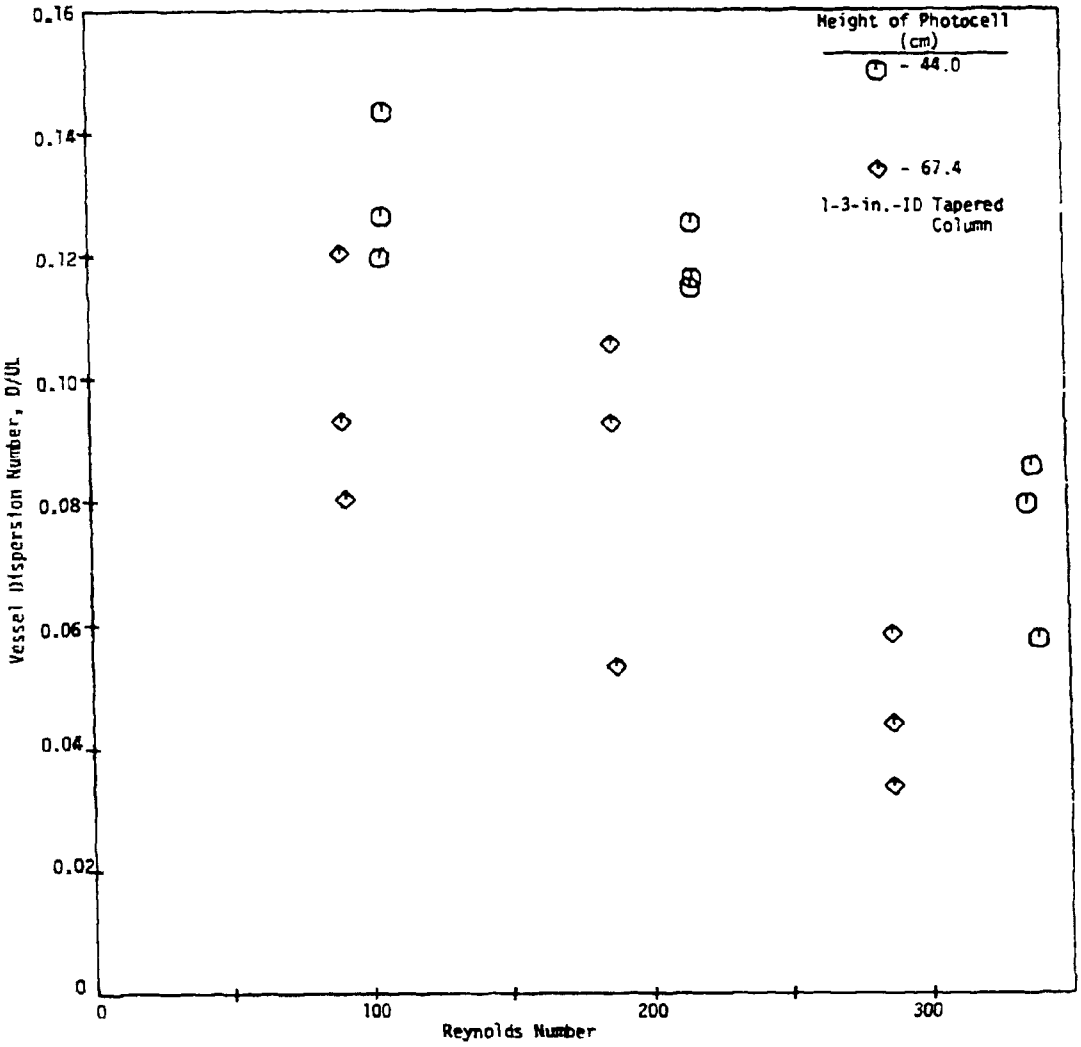

Fig. 13. Effect of Reynolds Number on Vessel Dispersion Number

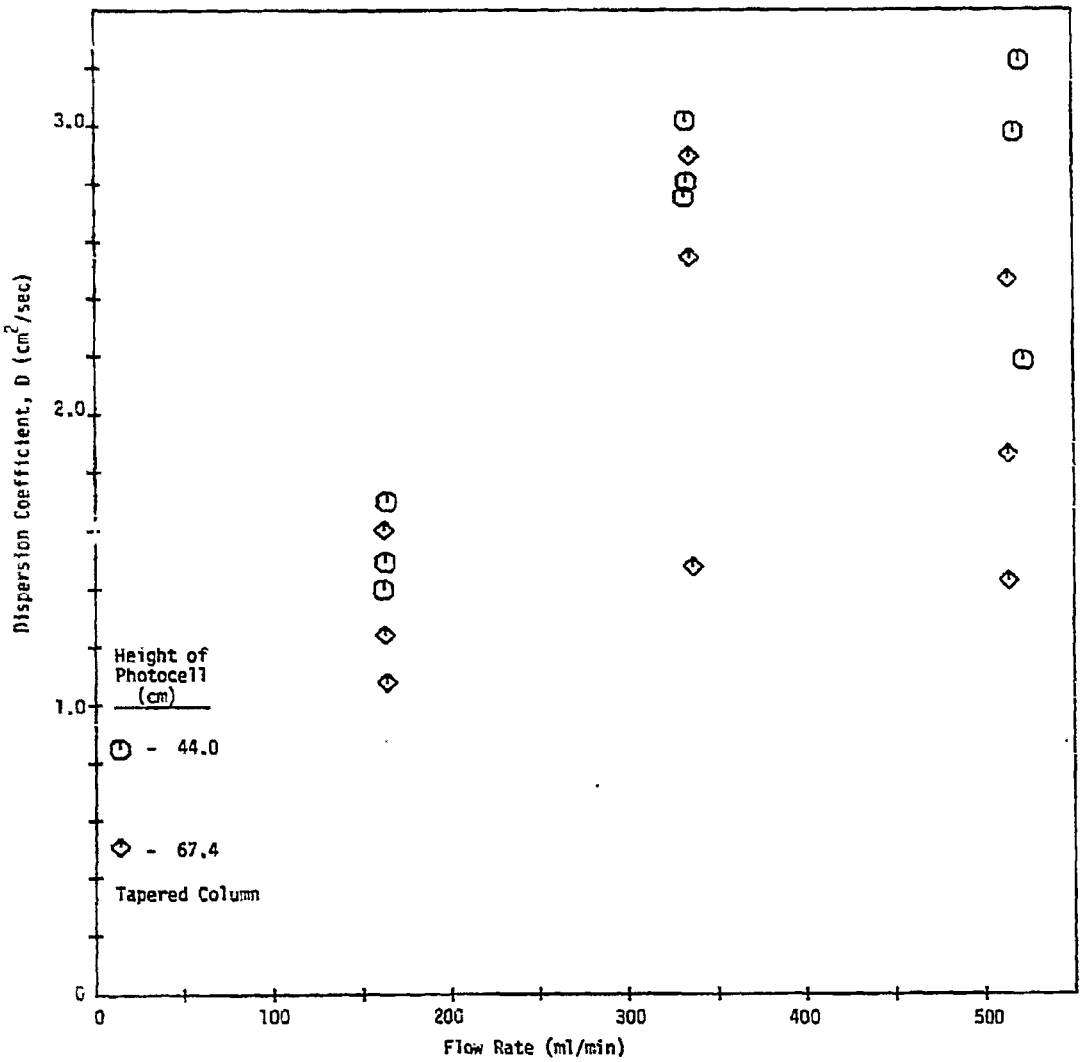

Fig. 14. Effect of Flow Rate on Dispersion Coefficient

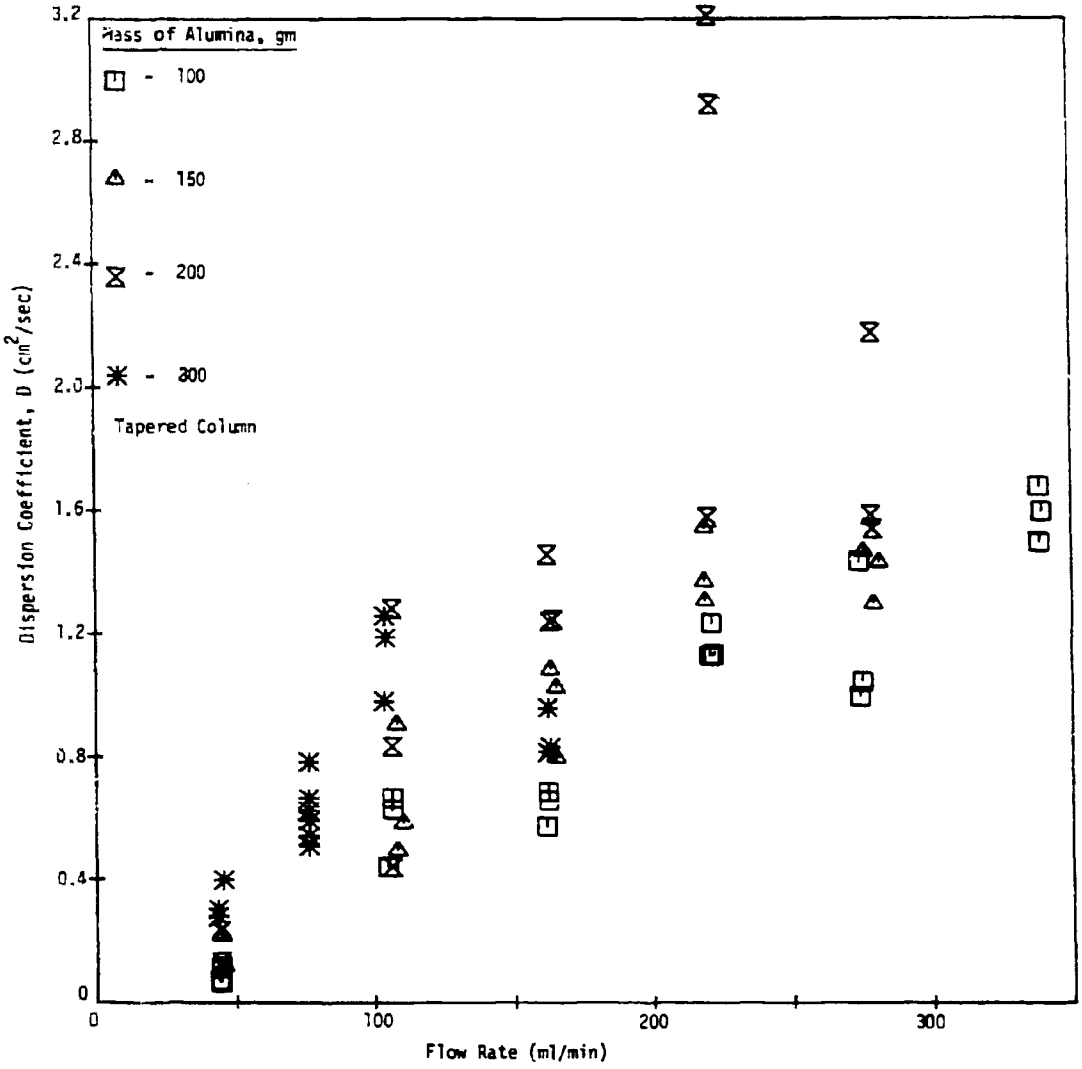

Fig. 15. Effect of Flow Rate on Dispersion Coefficient for Alumina

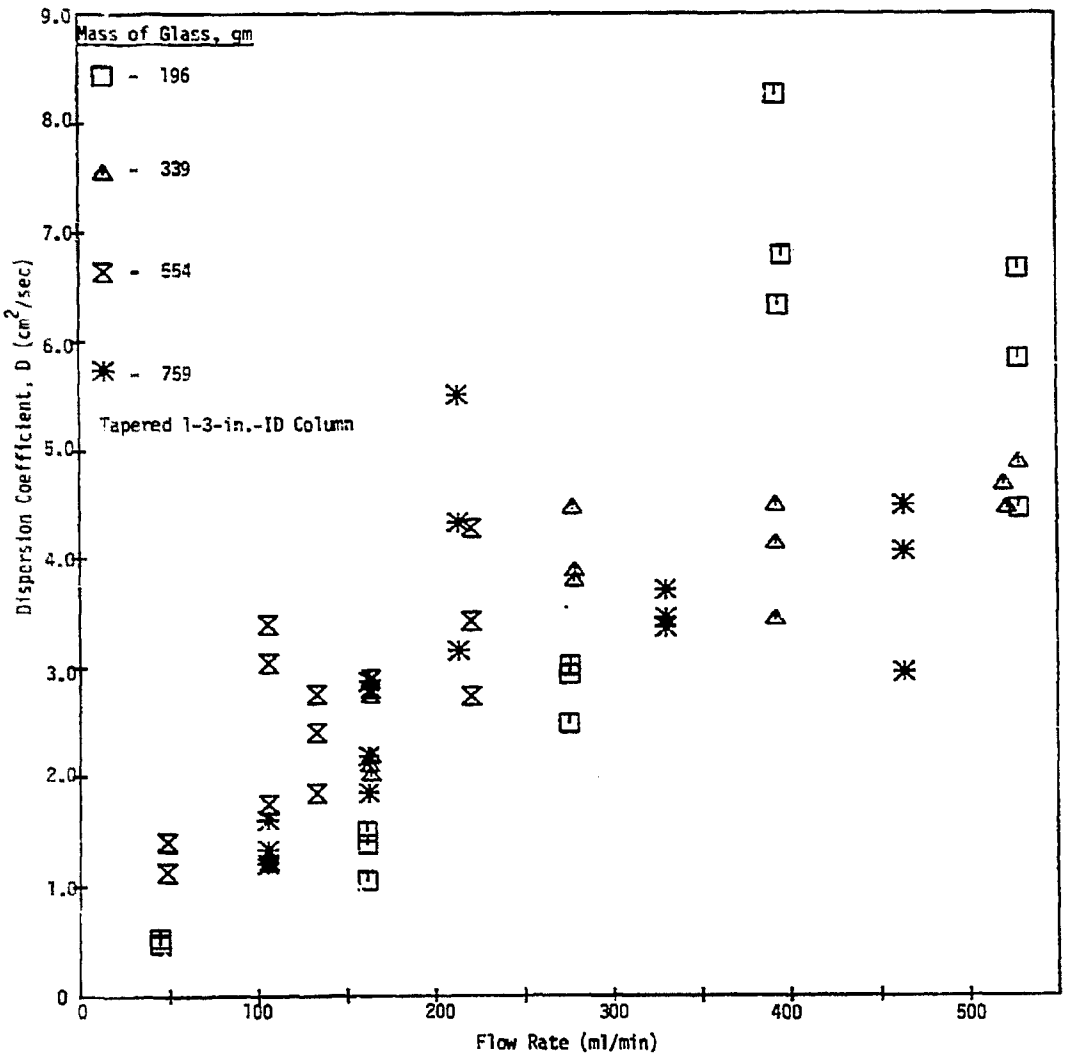

Fig. 16. Effect of Flow Rate on Dispersion Coefficient for Glass

therefore, fluidized bed height. For all flow rates the dispersion coefficients for 196 and 339 g of glass were greater than those for 200 and 300 g of alumina, and all the fluidized bed heights of alumina were much greater than the heights for glass.

The inverse Peclet number decreased with increasing Reynolds number as shown in Fig. 17 for two bed heights in the liquid tapered column. As observed in the empty 2-in. cylindrical column, the pattern of this decrease follows the pattern of an extrapolation of Taylor's theoretical curve for turbulent flow into the laminar regime (Fig. 2). This indicates that dispersion similar to that expected in a turbulent regime may also occur at low Reynolds number. This turbulence might result from eddies near the column entrance, where there is a sudden expansion of cross-sectional area from the inlet tube area to the area of the bottom of the column. Since the trend of increasing inverse Peclet number with increasing Reynolds number, shown in Fig. 2, is true only for fully-developed laminar flow, one would not expect the same trend in Fig. 17.

4.2 Theoretical Results

The differential mass balance equation for a tapered bed is found (see Appendix 8.3) to be

$$\frac{Fh^2}{\pi R^2 (Z+H_o)^2}\frac{\partial C}{\partial Z} - \frac{2D}{Z+H_o}\frac{\partial C}{\partial Z} - D\frac{\partial^2 C}{\partial Z^2} = -\frac{\partial C}{\partial t} \tag{27}$$

with boundary conditions

$$D\frac{\partial C}{\partial Z}(t, 0) = 0 \tag{28}$$

$$C(t, \infty) = 0 \tag{29}$$

$$C(0, Z) = 0 \tag{30}$$

$$C(0, 0) = \infty \tag{31}$$

$$\int_0^\infty CA\,dZ = 1 \tag{32}$$

The stagnant fluid dispersion model (assuming zero velocity) in dimensionless form is

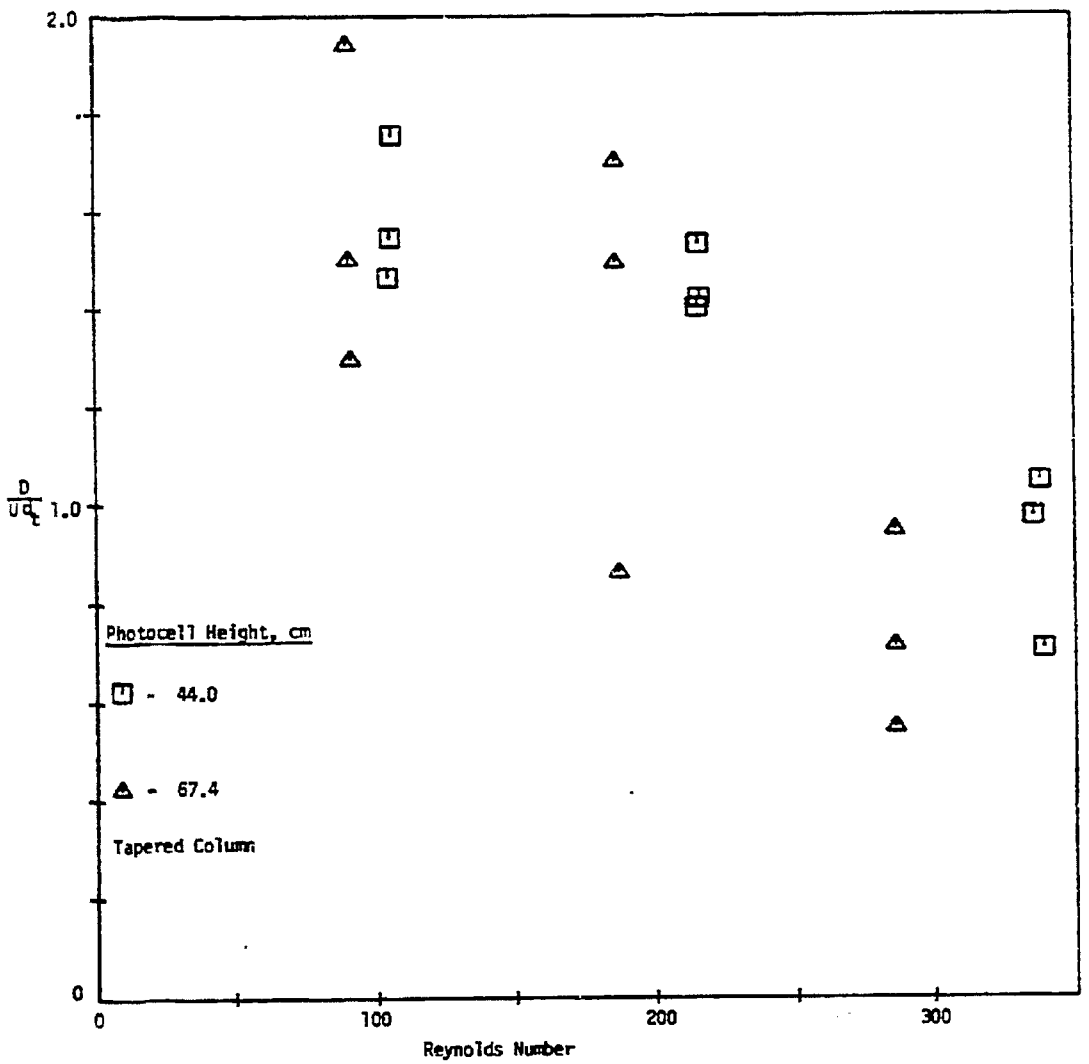

Fig. 17. Effect of Reynolds Number on Inverse Peclet Number

$$\frac{\partial^2 C}{\partial Z^2} + \frac{2D}{\ell}\frac{\partial C}{\partial Z} = D'\frac{\partial C}{\partial \theta} \tag{33}$$

By Laplace transform, Bessel's equation was obtained and the solution is

$$\bar{C}(x) = x^{-1/2}[A_0 I_{1/2}(x) + B_0 i_{-1/2}(x)] \tag{34}$$

With transformed boundary conditions

$$\bar{C}(\infty) = 0 \tag{35}$$

$$\bar{C}(0) = 1 \tag{36}$$

$$\frac{\partial \bar{C}}{\partial x}(0) = 0 \tag{37}$$

$$L\left[\int_0^\infty C A dx\right] = \int_0^\infty \bar{C} A dx = \frac{1}{p} \tag{38}$$

The application of boundary conditions (36) and (38) to Eq. (34) is shown in Appendix 8.3. However, a mathematical difficulty was encountered in evaluating the constants A_0 and B_0. Although attempts have been made to integrate Eq. (38) analytically to evaluate constants A_0 and B_0, it is suspected that the integral cannot be evaluated analytically.

If A_0 and B_0 can be evaluated, $\bar{C}$ will be expressed as a function of x and p. The variance of the concentration-time function is related to the derivatives of $\bar{C}$ with respect to p by Eq. (25). When these derivatives are evaluated, the variance can then be related to the dispersion coefficient.

5. CONCLUSIONS

1. As previously predicted by the Levenspiel model, the vessel dispersion number decreased with an increase in flow rate for both the cylindrical and the tapered columns with and without solids.

2. The dispersion coefficient in a tapered column is a function of flow rate and bed height.

3. The dispersion coefficients were greater for glass than for alumina in the tapered column.

4. The model for increased Peclet number in the laminar regime, as correlated by Levenspiel, does not apply to the vessels studied.

5. The inverse Peclet number decreases with increasing flow rate for both tapered and cylindrical columns with and without solids.

6. The dispersion coefficient increased with increasing flow rate for both cylindrical and tapered column with and without solids.

6. RECOMMENDATIONS

1. Operator errors which may have occurred during the manual injection procedure can be avoided by replacing the regular three-way valves with three-way solenoid valves.

2. More accurate calculation of the variances, less time for processing the C-curves, and more efficient data collection can be achieved if a digital computer is programmed to record the voltage readings directly from the voltmeter.

3. A second photocell located at the entrance of the vessel being studied would enable measurement of the variance of the tracer input.

7. ACKNOWLEDGMENT

The authors wish to thank C.W. Hancher and G.B. Dinsmore for their help and advice.

8. APPENDIX

8.1 The Effective Diameter of a Conical Section

The effective diameter is calculated by equating the volume of a section of height, Z, in the tapered column to the volume of a cylinder of equal height, as shown in Fig. 18. The volume of the conical section is

$$V_{tap} = \frac{1}{3}\pi r^2(H_o + Z) - \frac{1}{3}\pi r_o^2 H_o \qquad (39)$$

From the actual dimensions of the experimental tapered column (in cm),

$$r = r_o + \frac{Z}{h}(R - r_o) = 1.27 + 0.0229\ Z \qquad (40)$$

If Eq. (40) and the constants H_o and r_o are substituted into Eq. (39),

$$V_{tap} = \frac{1}{3}\pi(1.27 + 0.0229\ Z)^2\ (Z + 55.2) - 93.3 \qquad (41)$$

If the volume of the desired cylinder of height Z is set equal to the volume of the tapered section,

$$V_{cyl} = \frac{\pi}{4}(d_{eff})^2 Z = V_{tap} \qquad (42)$$

The effective diameter is then

$$d_{eff} = 2\left(\frac{V_{tap}}{\pi Z}\right)^{1/2} \qquad (43)$$

8.2 Sample Calculations

Sample calculations are shown for experiment 34. The tapered column was charged with 300 g of -70+100 mesh alumina having a wet density of one g/cm^3. The flow rate was 43.7 ml/min and static bed height was 33.5 cm. The chart speed was 0.5 in./min and an attenuation of 5 v was used. For readings taken at equal time intervals (Δt_i = const), the mean time is calculated by Eq. (5) with chart speed of 0.5 in./min:

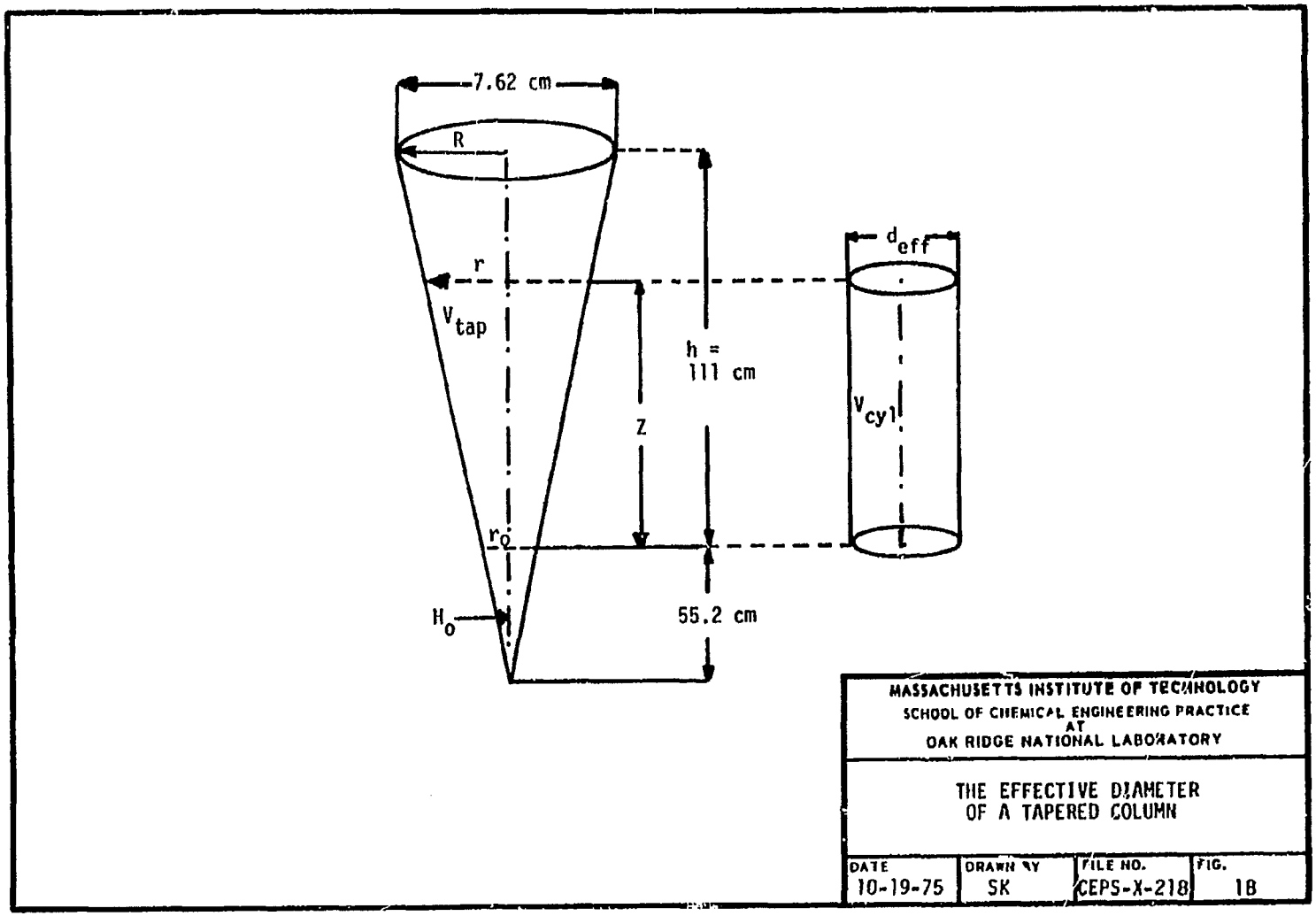

MASSACHUSETTS INSTITUTE OF TECHNOLOGY SCHOOL OF CHEMICAL ENGINEERING PRACTICE AT OAK RIDGE NATIONAL LABORATORY			
THE EFFECTIVE DIAMETER OF A TAPERED COLUMN			
DATE 10-19-75	DRAWN BY SK	FILE NO. CEPS-X-218	FIG. 18

$$\bar{t} \cong \frac{(3x0) + (3x1) + (3x2) + (3x3) + (10x4) + (22x5) + (35x6) + \ldots}{3 + 3 + 3 + 3 + 10 + 22 + 35 + \ldots}$$

$$\cong 11.06 \text{ min}$$

The variance is calculated by Eq. (8):

$$\sigma^2 = \frac{0^2x3 + 1^2x3 + 2^2x3 + 3^2x3 + 4^2x10 + 5^2x22 + 6^2x35 + \ldots}{3 + 3 + 3 + 3 + 10 + 22 + 35 + \ldots}$$

$$-(11.06)^2 = 21.09$$

This variance is substituted into Eq. (15) and solved for D/UL by an iterative technique.

$$\frac{(21.09)^2}{(11.06)^2} = 2\left(\frac{D}{UL}\right) - 2\left(\frac{D}{UL}\right)^2\left(1 - e^{UL/D}\right)$$

From the iterative program,

$$\frac{D}{UL} = 0.0952$$

The effective diameter is calculated by Eq. (43)

$$d_{eff} = 2\left[\frac{\frac{1}{3}x3.14(1.27 + 0.0229x44.4)^2 \times (44.4 + 55.22) - 93.3}{3.14 \times 44.4}\right]^{1/2} \quad (44)$$

$$= 3.58 \text{ cm}$$

From Eq. (45) the effective superficial velocity is

$$U_{eff} = \frac{43.7 \text{ cm}^3/\text{min}}{60 \text{ sec/min}(3.58 \text{ cm}/4)^2 3.14} = 0.072 \text{ cm/sec} \quad (45)$$

The dispersion coefficient is then found by multiplication of U_{eff} by bed height and by the vessel dispersion number:

$$D = (0.072 \text{ cm/sec})(44.4 \text{ cm})(0.0952) = 0.303 \text{ cm}^2/\text{sec}$$

The inverse Peclet number is:

$$\frac{1}{Pe} = \frac{0.303}{(0.072)(3.58)} = 1.174$$

8.3 Location of Data

The original data are located in ORNL Databooks A-7220-G, pp. 74-104, and A-7548-G, pp. 1-37. The databooks and calculations are on file at the MIT School of Chemical Engineering Practice, Bldg. 3001, ORNL.

8.4 Nomenclature

A	vessel area, cm^2
C	concentration of tracer
C_θ	concentration at dimensionless time
d	tube diameter
d_{eff}	effective diameter, cm
d_t	diameter of vessel, cm
D	dispersion coefficient, cm^2/sec
D_L'	effective dispersion coefficient, cm^2/sec
D_v	molecular diffusion coefficient, cm^2/sec
F	flow rate, cc/min
h	height of vessel, cm
H_o	height of cone, cm
L	length of vessel, cm
Pe	Peclet number, Ud_t/D
r	radius of vessel, cm
R	radius at top of vessel, cm

Re	Reynolds number, $\rho U d_t / \mu$
Sc	Schmidt number, $\mu / \rho D_v$
t	time, sec
t_o	initial time, sec
$\bar{t}$	mean time, sec
U	superficial velocity, cm/sec
U_{eff}	effective average superficial velocity, cm/sec
V	volume of vessel, cc
V_{cyl}	volume of cylindrical column, cc
V_{tap}	volume of tapered column, cc
Z	axial distance, cm

Greek Symbols

ϵ	roughness coefficient, cm
σ^2	variance, min^2
ρ	density of liquid
θ	dimensionless time
μ	viscosity of liquid

8.5 Literature References

1. Aris, R., Proc. Royal Soc., A235, 67 (1956).

2. Aris, R., "Letter to the Editor - Notes on the Diffusion-Type Model for Longitudinal Mixing Inflow (Levenspiel, Smith and Van der Laar)," Chem. Eng. Sci., 9, 266 (1959).

3. Bischoff, K.B., "Letter to the Editors - Notes on the Diffusion-Type Model for Longitudinal Mixing Inflow," Chem. Eng. Sci., 12, 69 (1960).

4. Bischoff, K.B., and O. Levenspiel, "Fluid Dispersion-Generalization and Comparison of Mathematical Models - I. Generalization of Models," Chem. Eng. Sci., 17, 245 (1962).

5. Cairns, E.J., and J.M. Prausnitz, "Longitudinal Mixing in Fluidization," A.I.Ch.E. Journal, 6, 400 (1960).

6. Charles, M., R.W. Coughlin, B.R. Allen, E.K. Parachuri, and F.X. Hasselberger, "Lactase Immobilized on Stainless Steel and Other Dense Metal Oxide Supports," in "Immobilized Biochemicals and Affinity Chromatography," R.B. Dunlap, ed., pp. 213-234, Plenum Press, New York (1974).

7. Hancher, C.W., personal communication, ORNL (1975).

8. Hasselberger, F.X., B.R. Allen, E.K. Paruchuri, M. Charles, and R.W. Coughlin, Biochem. Biophys. Res. Commun., 57, 1054 (1974).

9. Levenspiel, O., "Longitudinal Mixing of Fluids Flowing in Circular Pipes," Ind. Eng. Chem., 50, 343 (1958).

10. Levenspiel, O., "Chemical Reaction Engineering," 2nd ed., p. 277, Wiley, New York (1972).

11. Levenspiel, O., and W.K. Smith, "Notes on the Diffusion-Type Model for the Longitudinal Mixing of Fluids in Flow," Chem. Eng. Sci., 6, 227 (1957).

12. Levey, R.P., Jr., A. de la Garza, S.C. Jacobs, H.M. Heidt, and P.E. Trent, "Fluid Bed Conversion of UO_3 to UF_4," Chem. Eng. Progr., 56(3), 43 (1960).

13. Scott, C.D., C.W. Hancher, and S.E. Shumate, III, "A Tapered Fluidized Bed as a Bioreactor," Enzyme Engineering Conference III, Plenum Press, in press.

14. Taylor, G., "Dispersion of Soluble Matter in Solvent Flowing Slowly Through a Tube," Proc. Royal Soc., A219, 186 (1953).

15. Taylor, G., "Conditions Under Which Dispersion of a Solute in a Stream of Solvent Can Be Used to Measure Molecular Diffusion," Proc. Royal Soc., A225, 473 (1954).

16. Van der Laar, E. Th., "Letter to the Editors - Notes on the Diffusion-Type Model for the Longitudinal Mixing in Flow (O. Levenspiel and W.K. Smith)," Chem. Eng. Sci., 7, 187 (1957).

SATISFACTION GUARANTEED

NTIS strives to provide quality products, reliable service, and fast delivery. Please contact us for a replacement within 30 days if the item you receive is defective or if we have made an error in filling your order.

▲▲ E-mail: info@ntis.gov
▲▲ Phone: 1-888-584-8332 or (703)605-6050

Reproduced by NTIS

National Technical Information Service
Springfield, VA 22161

This report was printed specifically for your order from nearly 3 million titles available in our collection.

For economy and efficiency, NTIS does not maintain stock of its vast collection of technical reports. Rather, most documents are custom reproduced for each order. Documents that are not in electronic format are reproduced from master archival copies and are the best possible reproductions available.

Occasionally, older master materials may reproduce portions of documents that are not fully legible. If you have questions concerning this document or any order you have placed with NTIS, please call our Customer Service Department at (703) 605-6050.

About NTIS

NTIS collects scientific, technical, engineering, and related business information – then organizes, maintains, and disseminates that information in a variety of formats – including electronic download, online access, CD-ROM, magnetic tape, diskette, multimedia, microfiche and paper.

The NTIS collection of nearly 3 million titles includes reports describing research conducted or sponsored by federal agencies and their contractors; statistical and business information; U.S. military publications; multimedia training products; computer software and electronic databases developed by federal agencies; and technical reports prepared by research organizations worldwide.

For more information about NTIS, visit our Web site at **http://www.ntis.gov**.

NTIS

Ensuring Permanent, Easy Access to U.S. Government Information Assets

U.S. DEPARTMENT OF COMMERCE
Technology Administration
National Technical Information Service
Springfield, VA 22161 (703) 605-6000